applied sciences

MDPI

Article

A Never-Ending Conformational Story of the Quercetin Molecule: Quantum-Mechanical Investigation of the O3′H and O4′H Hydroxyl Groups Rotations

Ol'ha O. Brovarets' [1,*] and Dmytro M. Hovorun [1,2]

[1] Department of Molecular and Quantum Biophysics, Institute of Molecular Biology and Genetics, National Academy of Sciences of Ukraine, 150 Akademika Zabolotnoho Street, 03680 Kyiv, Ukraine; dhovorun@imbg.org.ua

[2] Department of Molecular Biotechnology and Bioinformatics, Institute of High Technologies, Taras Shevchenko National University of Kyiv, 2-h Akademika Hlushkova Avenue, 03022 Kyiv, Ukraine

* Correspondence: o.o.brovarets@imbg.org.ua

Received: 8 January 2020; Accepted: 2 February 2020; Published: 8 February 2020

Abstract: The quercetin molecule is known to be an effective pharmaceutical compound of a plant origin. Its chemical structure represents two aromatic A and B rings linked through the C ring containing oxygen and five OH hydroxyl groups attached to the 3, 3′, 4′, 5, and 7 positions. In this study, a novel conformational mobility of the quercetin molecule was explored due to the turnings of the O3′H and O4′H hydroxyl groups, belonging to the B ring, around the exocyclic C-O bonds. It was established that the presence of only three degrees of freedom of the conformational mobility of the O3′H and O4′H hydroxyl groups is connected with their concerted behavior, which is controlled by the non-planar (in the case of the interconverting planar conformers) or locally non-planar (in other cases) $TSs^{O3'H/O4'H}$ transition states, in which O3′H and O4′H hydroxyl groups are oriented by the hydrogen atoms towards each other. We also explored the number of the physico-chemical and electron-topological characteristics of all intramolecular-specific contacts—hydrogen bonds and attractive van der Waals contacts at the conformers and also at the transition states. Long-terms perspectives for the investigations of the structural bases of the biological activity of this legendary molecule have been shortly described.

Keywords: Quercetin molecule; conformational mobility; hydroxyl group; transition state; concerted rotation of the hydroxyl groups; quantum-chemical calculations; quantum technology

1. Introduction

The quercetin molecule (3, 3′, 4′, 5, 7—pentahydroxyflavone, $C_{15}H_{10}O_7$) is an important flavonoid compound, which is found in many foods and plants, in particular in honey [1], and is known to act as a natural drug molecule with a wide range of treatment properties—antioxidant, anti-toxic, etc.—and is also involved in drug delivery from the site of administration to the therapeutic target [2–9]. The structure of the quercetin contains two aromatic A and B rings linked through the C ring containing oxygen and five OH hydroxyl groups attached to the 3, 3′, 4′, 5 and 7 positions (see Scheme 1) [10–15].

In a previous study [16], by using the quantum-mechanical (QM) calculations at the MP2/6-311++G(2df,pd)//B3LYP/6-311++G(d,p) level of QM theory together with Bader's "Quantum Theory of Atoms in Molecules", for the first time, all possible conformers were established, corresponding to local minima on the potential energy hypersurface of the isolated quercetin molecule.

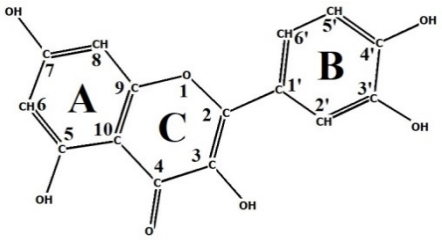

Scheme 1. Chemical structure of the quercetin molecule and standard numeration of its atoms.

Altogether, 48 stable conformers were established, which have been divided into four different conformational subfamilies by their structural properties: subfamily I—conformers **1**–**12**; subfamily II—conformers **13-18**, **20**, **23**, **24**, **26**, **29**, and **30**; subfamily III—conformers **19**, **21**, **22**, **25**, **27**, **28**, and **31**–**36**; subfamily IV—conformers **37**–**48** [16]. It was shown that these 48 stable conformers (24 planar structures (C_s point symmetry) and 24 non-planar structures (C_1 point symmetry)) represent a comprehensive set of the theoretically possible structures.

Conformers of quercetin are polar structures with a dipole moment, which varies within the range from 0.35 to 9.87 Debye for different conformers with different direction for each.

Their relative Gibbs free energies are arranged within the range from 0.00 to 25.30 kcal·mol^{-1} under normal conditions in vacuum.

One half of these structures (24 conformers) possesses planar structure (C_s point symmetry), whereas the other half (24 conformers) does not have symmetry at all (C_1 point symmetry) (C3C2C1′C2′ = 40.9–44.3 degree; C2C3O3H = 9.4–16.3 degree).

We also defined their physico-chemical characteristics, in particular, structural, energetic, and polar, which are necessary for understanding of the biological mechanisms of action of this molecule. Intramolecular specific contacts have also been explored in detail.

Bader's "Quantum Theory of Atoms in Molecules" analysis shows that conformers of the quercetin molecule differ from each other by the intramolecular specific contacts (two or three), stabilizing all possible conformers of the molecule—H-bonds (both classical OH … O and so-called unusual CH … O and OH … C) and attractive van der Waals contacts O … O. Energies of these cooperative intramolecular specific contacts have been estimated [16].

Also, it was theoretically modeled the conformational interconversions [17–21] in the 24 pairs of the conformers of the quercetin molecule through the rotation of its almost non-deformable (A+C) and B rings around the C2-C1′ bond through the quasi-orthogonal transition state (TS) with low values of the imaginary frequencies (28-33/29-36 cm^{-1}) and Gibbs free energies of activation in the range of 2.17 to 5.68/1.86 to 4.90 kcal·mol^{-1} in the continuum with dielectric permittivity $\varepsilon = 1/\varepsilon = 4$ under normal conditions. Also, we studied the changes of the number of physico-chemical characteristics of all intramolecular specific contacts—hydrogen bonds and attractive van der Waals contacts during these conformational rearrangements.

This study is a logical development of the previous investigations [16–18] and is devoted to the novel interconversions between the conformers of the quercetin molecule due to the rotations of the O3′H and O4′H hydroxyl groups around the exocyclic C-O bonds outside.

As a result, it was found that different conformers of the quercetin molecule are tightly interconnected with each other through the set of the TSs. Moreover, these conformational transformations are assisted by the intramolecular H-bonds and van der Waals contacts.

In reality, it is not as easy a task as it seems, as the question of "Why two neighboring hydroxyl groups in the aromatic ring have only three, but not four conformational degrees of freedom?" remains without answer [22,23].

The main idea of this investigation is summarized in the following statements.

We suggest that the conformational mobility of the C ring of the quercetin molecule, which contains two neighboring O3′H and O4′H hydroxyl groups, that is, conversion of one stable

O3'HO4'H/O4'HO3'H configuration into the other O4'HO3'H/O3'HO4'H and *vice versa*, is realized by two significantly different pathways from the topological and energetical point of view.

First, (this pathway is more or less evident) it occurs by the restricted rotations of the hydroxyls by the angle of 180 degrees through the corresponding TSs and through the high-energetical dynamically stable O3'HO4'H/O4'HO3'H configuration. The other pathway is quite unusual—it is realized through one conformational transition, which has concerted character and is controlled by the non-planar $TSs^{O3'HHO4'/O4'HHO3'}$ with the high values of the imaginary frequency.

A previously suggested idea has been completely confirmed by careful QM investigation—we have identified for the first time the aforementioned pathways of the conformational variability of the quercetin molecule and documented their structural properties, including symmetrical, polar, energetical, and kinetic characteristics, which are quite important for the understanding of the structural grounds of the biological activity of the quercetin molecule.

2. Computational Methods

Calculations of the geometrical structures of the TSs of the conformational interconversions and their vibrational spectra, corresponding to the local minima on the potential (electronic) energy hyper surface, have been performed at the DFT B3LYP/6-311++G(d,p) level of QM theory [24–26] by Gaussian'09 program package [27], which was successfully approved in our previous studies for the calculations of the heterocyclic compounds [28,29]. A scaling factor of 0.9668 has been used to correct the harmonic frequencies for the investigated structures [30]. Intrinsic reaction coordinate (IRC) calculations in the forward and reverse directions from each TS, which have been confirmed by the presence of one and only one imaginary frequency in the vibrational spectra, have been performed using Hessian-based predictor–corrector integration algorithm [31].

All calculations were performed for the quercetin molecule as their intrinsic property, that is adequate for modeling of the processes occurring in real systems [16,17,32].

Electronic and Gibbs free energies under normal conditions have been calculated by single point calculations at the MP2/6-311++G(2df,pd) level of theory [33–35].

The time $\tau_{99.9\%}$ necessary to reach 99.9% of the equilibrium concentration of the reactant and product in the system of the reversible first-order forward (k_f) and reverse (k_r) reactions can be estimated by the formula [36]

$$\tau_{99.9\%} = \frac{ln10^3}{k_f + k_r} \quad (1)$$

The lifetime, τ, of the conformers has been calculated using the formula $1/k_r$, where the values of the forward k_f and reverse k_r rate constants for the tautomerization reactions were obtained as [36]

$$k_{f,r} = \Gamma \cdot \frac{k_B T}{h} e^{-\frac{\Delta\Delta G_{f,r}}{RT}} \quad (2)$$

where the quantum tunneling effect has been accounted by Wigner's tunneling correction [37], successfully used for the double proton reactions in DNA base pairs [28]:

$$\Gamma = 1 + \frac{1}{24}\left(\frac{h\nu_i}{k_B T}\right)^2 \quad (3)$$

where k_B—Boltzmann's constant, h—Planck's constant, $\Delta\Delta G_{f,r}$—Gibbs free energy of activation for the conformational transition in the forward (f) and reverse (r) directions, and ν_i—magnitude of the imaginary frequency associated with the vibrational mode at the TS.

The topology of the electron density was analyzed using the program package AIM'2000 [38] with all default options and wave functions obtained at the level of theory used for geometry optimization. The presence of the (3,−1) bond critical point (BCP), bond path between hydrogen donor and acceptor,

and positive value of the Laplacian at this BCP ($\Delta\rho > 0$) were considered altogether as criteria for the formation of the H-bond and attractive van der Waals contact [39].

In this work, standard numeration of atoms has been used [16,17]. Numeration of the conformers, which are highlighted in bold in the text, have been used as in the work [16].

3. Obtained Results and Their Discussion

In this study, we logically continued to investigate the conformational mobility [16–18] of the quercetin molecule and extend this approach to the rotations of the hydroxyl groups in the 3′ and 4′ positions, which are carefully presented in Tables 1–3 and Figures 1–3. The most obvious methods of the conformational interconversions between the 48 conformers [16] of the quercetin molecule were considered and investigated in detail through the rotations of the O3′H and O4′H hydroxyl groups around the exocyclic C-O covalent bonds. In this case, the TSs have been formed gradually, starting from the 48 conformers of the quercetin molecule [16] by the single or concerted rotations of the O3′H and O4′H hydroxyl groups—designated as $TS^{O3'H}$, $TS^{O4'H}$, and $TS^{O3'H/O4'H}$, respectively.

Therefore, detailed analysis of the obtained results enabled us to obtain the following observations and their discussion. As individual, the concerted rotational transitions of the O3′H and O4′H hydroxyl groups proceed through the mirror-symmetrical pathways, which are controlled by the mirror-symmetrical TSs. Totally, we have revealed 48 TSs—16 TSs in each case (Figures 1–3; Tables 1–3).

Individual conformational transitions are controlled by the non-planar $TS^{O3'H}$ and $TS^{O4'H}$ (C_1 point symmetry) with non-orthogonal structure (see HO3′C3′C2′ (78.7–83.3 degree) and HO4′C4′C5′ (80.2–82.1 degree) dihedral angles in Tables 1 and 2 and Figures 1 and 2). Their non-orthogonal structure, most probably, could be connected with the non-symmetrical surrounding of the free electronic pairs of the oxygen atoms of the hydroxyl groups. The TSs for the concerted conformational transformations—$TSs^{O3'H/O4'H}$—possess non-planar structure in the case of the planar conformers **1**-**12**, **19**, **21**, **22**, **25**, **27**, **28**, and **31**–**36** and local non-planar structure for the non-planar conformers, **13**-**18**, **20**, **23**, **24**, **26**, **29**, **30**, and **37**–**48**, which mutually interconvert (Figure 3, Table 3).

Gibbs free energies of activation for these processes form the following order; $\Delta\Delta G_{TS}{}^{O4'H}$ (3.33–7.05) < $\Delta\Delta G_{TS}{}^{O3'H}$ (4.23–7.08) < $\Delta\Delta G_{TS}{}^{O3'H/O4'H}$ (4.41–7.56 kcal·mol^{-1} under normal conditions) (Tables 1–3). The imaginary frequencies are in the following ranges: 366.7–391.5 ($TS^{O3'H}$), 328.8–363.5 ($TS^{O4'H}$), and 454.5–483.1 ($TS^{O3'H/O4'H}$). Without exception, 48 conformers of the quercetin molecule have been established to be the dynamically stable structures, based on the investigated conformational transitions. During their lifetime (τ = (1.05–2.53)·10^{-11} s) (Tables 1–3), the lowest frequency intramolecular vibrations can occur [16].

It is a characteristic feature that investigated conformational transitions are dipole-active, as they cause the changing of the dipole moment by the absolute value, so by the spatial orientation, and practically do not disturb the structure of the quercetin molecule and physico-chemical characteristics of its specific intramolecular interactions. Even the energy of the intramolecular C2′/C6′H … O3 and O3H … C2′/C6′H H-bonds between the B and C rings (Figures 1–3) change at these conformational transitions by no more than on ~4.7%. Interestingly, concerted conformational transitions, which are controlled by the $TSs^{O3'H/O4'H}$, proceed without intermediates on the hyperspace of the Gibbs free energy.

Moreover, we did not register any specific intramolecular interactions in the B ring of the quercetin molecule at the conformational motions of the O3′H and O4′H hydroxyl groups. All investigated conformational transitions are quite rapid processes, for which $1.04 \cdot 10^{-10} > \tau_{99.9\%} > 7.30 \cdot 10^{-11}$ s.

Therefore, provided investigation gives total assurance that the availability of the three conformational degrees of freedom for the O3′H and O4′H hydroxyl groups is connected with their concerted, coordinated behavior (Figure 3, Table 3).

Let us to make one important notion before going to the conclusions. It is known, that biological activity of the molecules, is caused by at least two interdependent reasons—their intramolecular structural variability and specific interaction with the targets of the different origin.

Table 1. Energetic, polar, structural, and kinetic characteristics of the conformational transitions in the isolated quercetin molecule via the mirror-symmetrical rotations of the O3′H hydroxyl group around the C3′-O3′ bond through the transition states (TSs) with a non-perpendicularly-oriented O3′H group, obtained at the MP2/6-311++G(2df,pd)//B3LYP/6-311++G(d,p) level of QM theory under normal conditions (see Figure 1).

TS of the Conformational Transition	μ_{TS} [a]	ν_i [b]	ΔG [c]	ΔE [d]	$\Delta\Delta G_{TS}$ [e]	$\Delta\Delta E_{TS}$ [f]	$\Delta\Delta G$ [g]	$\Delta\Delta E$ [h]	k_f [i]	k_r [j]	$\tau_{99.9\%}$ [k]	τ [l]	HO3′C3′C2′ [m]
$TS^{O3'H}{}_{2\leftrightarrow9}$	1.78	340.2	3.98	3.80	6.90	6.75	2.91	2.95	$6.01\cdot10^{7}$	$5.01\cdot10^{10}$	$1.38\cdot10^{-10}$	$2.00\cdot10^{-11}$	±80.1
$TS^{O3'H}{}_{4\leftrightarrow11}$	4.02	333.4	4.15	4.07	7.08	6.73	2.93	2.66	$4.36\cdot10^{7}$	$4.82\cdot10^{10}$	$1.43\cdot10^{-10}$	$2.07\cdot10^{-11}$	±79.1
$TS^{O3'H}{}_{7\leftrightarrow10}$	4.10	361.1	3.29	3.21	6.25	6.53	2.97	3.32	$1.80\cdot10^{8}$	$4.62\cdot10^{10}$	$1.49\cdot10^{-10}$	$2.17\cdot10^{-11}$	∓82.8
$TS^{O3'H}{}_{8\leftrightarrow12}$	5.93	362.0	3.32	3.23	6.25	6.51	2.93	3.28	$1.80\cdot10^{8}$	$4.91\cdot10^{10}$	$1.40\cdot10^{-10}$	$2.04\cdot10^{-11}$	∓82.9
$TS^{O3'H}{}_{14\leftrightarrow24}$	5.08	355.2	3.70	3.75	6.50	6.92	2.80	3.17	$1.17\cdot10^{8}$	$6.09\cdot10^{10}$	$1.13\cdot10^{-10}$	$1.64\cdot10^{-11}$	±81.3
$TS^{O3'H}{}_{15\leftrightarrow26}$	6.24	340.9	3.79	3.97	6.47	6.86	2.68	2.89	$1.23\cdot10^{8}$	$7.44\cdot10^{10}$	$9.27\cdot10^{-11}$	$1.34\cdot10^{-11}$	∓79.3
$TS^{O3'H}{}_{17\leftrightarrow29}$	7.60	355.6	3.81	3.91	6.62	7.05	2.81	3.15	$9.70\cdot10^{7}$	$6.03\cdot10^{10}$	$1.14\cdot10^{-10}$	$1.66\cdot10^{-11}$	±80.6
$TS^{O3'H}{}_{18\leftrightarrow30}$	8.65	343.3	3.79	3.94	6.50	6.87	2.71	2.93	$1.17\cdot10^{8}$	$7.04\cdot10^{10}$	$9.79\cdot10^{-11}$	$1.42\cdot10^{-11}$	∓79.5
$TS^{O3'H}{}_{21\leftrightarrow34}$	3.08	328.8	4.01	4.14	6.54	6.70	2.53	2.56	$1.09\cdot10^{8}$	$9.51\cdot10^{10}$	$7.26\cdot10^{-11}$	$1.05\cdot10^{-11}$	±78.7
$TS^{O3'H}{}_{27\leftrightarrow33}$	6.23	363.5	3.25	3.03	6.27	6.29	3.02	3.27	$1.75\cdot10^{8}$	$4.25\cdot10^{10}$	$1.62\cdot10^{-10}$	$2.35\cdot10^{-11}$	∓83.3
$TS^{O3'H}{}_{31\leftrightarrow36}$	3.35	336.2	3.85	3.86	6.39	6.63	2.54	2.77	$1.42\cdot10^{8}$	$9.44\cdot10^{10}$	$7.30\cdot10^{-11}$	$1.06\cdot10^{-11}$	±79.8
$TS^{O3'H}{}_{32\leftrightarrow35}$	5.97	362.6	3.23	3.05	6.29	6.38	3.06	3.33	$1.69\cdot10^{8}$	$3.96\cdot10^{10}$	$1.74\cdot10^{-10}$	$2.53\cdot10^{-11}$	∓83.2
$TS^{O3'H}{}_{39\leftrightarrow45}$	6.15	354.7	3.83	3.92	6.60	7.01	2.77	3.09	$9.97\cdot10^{7}$	$6.43\cdot10^{10}$	$1.07\cdot10^{-10}$	$1.56\cdot10^{-11}$	±80.5
$TS^{O3'H}{}_{40\leftrightarrow46}$	7.86	344.1	3.70	3.82	6.45	6.80	2.75	2.98	$1.27\cdot10^{8}$	$6.60\cdot10^{10}$	$1.04\cdot10^{-10}$	$1.52\cdot10^{-11}$	±80.5
$TS^{O3'H}{}_{42\leftrightarrow48}$	6.37	341.6	3.70	3.85	6.41	6.79	2.71	2.94	$1.36\cdot10^{8}$	$7.05\cdot10^{10}$	$9.78\cdot10^{-11}$	$1.42\cdot10^{-11}$	∓79.6
$TS^{O3'H}{}_{44\leftrightarrow47}$	4.47	353.8	1.46	1.51	4.23	4.62	2.77	3.12	$5.47\cdot10^{9}$	$6.46\cdot10^{10}$	$9.85\cdot10^{-11}$	$1.55\cdot10^{-11}$	±81.1

[a] The dipole moment of the TS, Debye. [b] The imaginary frequency at the TS of the conformational transition, cm^{-1}. [c] The Gibbs free energy of the initial relative to the terminal conformer of the quercetin molecule (T = 298.15 K), $kcal\cdot mol^{-1}$. [d] The electronic energy of the initial relative to the terminal conformer of the quercetin molecule, $kcal\cdot mol^{-1}$. [e] The Gibbs free energy barrier for the forward conformational transformation of the quercetin molecule, $kcal\cdot mol^{-1}$. [f] The electronic energy barrier for the forward conformational transformation of the quercetin molecule, $kcal\cdot mol^{-1}$. [g] The Gibbs free energy barrier for the reverse conformational transformation of the quercetin molecule, $kcal\cdot mol^{-1}$. [h] The electronic energy barrier for the reverse conformational transformation of the quercetin molecule, $kcal\cdot mol^{-1}$. [i] The rate constant for the forward conformational transformation, s^{-1}. [j] The rate constant for the reverse conformational transformation, s^{-1}. [k] The time necessary to reach 99.9% of the equilibrium concentration between the reactant and the product of the reaction of the conformational transformation, s. [l] The lifetime of the product of the conformational transition, s. [m] The dihedral angle, which describes at the TS the orientation of the O3′H hydroxyl group relatively the B ring of the quercetin molecule, degree; sings "±" correspond to enantiomers.

Table 2. Energetic, polar, structural, and kinetic characteristics of the conformational transitions in the isolated quercetin molecule via the mirror-symmetrical rotations of the O4′H hydroxyl group around the C4′-O4′ bond through the transition states (TSs) with a non-perpendicularly-oriented O4′H group, obtained at the MP2/6-311++G(2df,pd)//B3LYP/6-311++G(d,p) level of QM theory under normal conditions (see Figure 2).

TS of the Conformational Transition	μ_{TS}	ν_i	ΔG	ΔE	$\Delta\Delta G_{TS}$	$\Delta\Delta E_{TS}$	$\Delta\Delta G$	$\Delta\Delta E$	k_f	k_r	$\tau_{99,9\%}$	τ	HO4′C4′C5′
$TS^{O4'H}{}_{1\leftrightarrow10}$	2.41	381.6	4.20	4.30	7.05	7.38	2.84	3.08	$4.75{\cdot}10^{7}$	$5.77{\cdot}10^{10}$	$1.20{\cdot}10^{-10}$	$1.73{\cdot}10^{-11}$	±81.1
$TS^{O4'H}{}_{3\leftrightarrow9}$	2.82	391.5	3.92	4.03	6.86	7.23	2.94	3.21	$6.60{\cdot}10^{7}$	$4.95{\cdot}10^{10}$	$1.39{\cdot}10^{-10}$	$2.02{\cdot}10^{-11}$	∓81.9
$TS^{O4'H}{}_{5\leftrightarrow12}$	3.63	379.7	4.24	4.37	6.93	7.35	2.69	2.98	$5.80{\cdot}10^{7}$	$7.41{\cdot}10^{10}$	9.32E-11	$1.35{\cdot}10^{-11}$	±80.8
$TS^{O4'H}{}_{6\leftrightarrow11}$	3.99	389.2	3.86	4.00	6.92	7.14	3.07	3.14	$5.90{\cdot}10^{7}$	$3.98{\cdot}10^{10}$	$1.73{\cdot}10^{-10}$	$2.51{\cdot}10^{-11}$	∓82.1
$TS^{O4'H}{}_{13\leftrightarrow24}$	4.78	375.8	4.07	4.13	6.81	7.22	2.74	3.09	$7.12{\cdot}10^{7}$	$6.89{\cdot}10^{10}$	$1.00{\cdot}10^{-10}$	$1.45{\cdot}10^{-11}$	∓80.4
$TS^{O3'H}{}_{16\leftrightarrow30}$	6.83	374.4	4.01	4.11	6.78	7.16	2.77	3.04	$7.42{\cdot}10^{7}$	$6.52{\cdot}10^{10}$	$1.06{\cdot}10^{-10}$	$1.53{\cdot}10^{-11}$	±80.7
$TS^{O4'H}{}_{19\leftrightarrow33}$	4.64	371.6	4.12	4.49	6.74	7.25	2.62	2.76	$7.98{\cdot}10^{7}$	$8.40{\cdot}10^{10}$	$8.22{\cdot}10^{-11}$	$1.19{\cdot}10^{-11}$	±80.2
$TS^{O4'H}{}_{20\leftrightarrow26}$	4.64	371.6	0.63	0.72	6.71	7.51	6.08	6.79	$8.36{\cdot}10^{7}$	$2.42{\cdot}10^{8}$	$2.12{\cdot}10^{-8}$	$4.13{\cdot}10^{-9}$	±80.2
$TS^{O4'H}{}_{22\leftrightarrow34}$	5.05	380.8	4.04	3.97	6.71	7.00	2.67	3.03	$8.43{\cdot}10^{7}$	$7.74{\cdot}10^{10}$	$8.91{\cdot}10^{-11}$	$1.29{\cdot}10^{-11}$	∓81.8
$TS^{O4'H}{}_{23\leftrightarrow29}$	7.10	375.3	0.55	0.60	3.33	3.73	2.78	3.13	$2.52{\cdot}10^{10}$	$6.41{\cdot}10^{10}$	$7.73{\cdot}10^{-11}$	$1.56{\cdot}10^{-11}$	∓80.7
$TS^{O4'H}{}_{25\leftrightarrow35}$	5.37	373.7	4.12	4.35	6.84	7.22	2.71	2.88	$6.77{\cdot}10^{7}$	$7.17{\cdot}10^{10}$	$9.62{\cdot}10^{-11}$	$1.39{\cdot}10^{-11}$	±80.5
$TS^{O4'H}{}_{28\leftrightarrow36}$	5.70	382.7	4.07	4.06	6.74	7.08	2.67	3.02	$7.99{\cdot}10^{7}$	$7.71{\cdot}10^{10}$	$8.95{\cdot}10^{-11}$	$1.30{\cdot}10^{-11}$	∓81.6
$TS^{O4'H}{}_{37\leftrightarrow45}$	6.56	369.1	4.03	4.05	6.75	7.11	2.72	3.06	$7.80{\cdot}10^{7}$	$7.09{\cdot}10^{10}$	$9.74{\cdot}10^{-11}$	$1.41{\cdot}10^{-11}$	∓80.4
$TS^{O4'H}{}_{38\leftrightarrow46}$	6.19	367.5	4.03	4.16	6.72	7.10	2.69	2.95	$8.14{\cdot}10^{7}$	$7.40{\cdot}10^{10}$	$9.32{\cdot}10^{-11}$	$1.35{\cdot}10^{-11}$	±80.2
$TS^{O4'H}{}_{41\leftrightarrow48}$	5.09	366.7	4.00	4.10	6.69	7.05	2.69	2.94	$8.64{\cdot}10^{7}$	$7.42{\cdot}10^{10}$	$9.30{\cdot}10^{-11}$	$1.35{\cdot}10^{-11}$	±80.4
$TS^{O4'H}{}_{43\leftrightarrow47}$	5.49	369.4	1.83	1.88	4.73	5.10	2.90	3.22	$2.37{\cdot}10^{9}$	$5.21{\cdot}10^{10}$	$1.27{\cdot}10^{-10}$	$1.92{\cdot}10^{-11}$	∓80.2

For designations see Table 1.

Table 3. Energetic, polar, structural, and kinetic characteristics of the conformational transitions in the isolated quercetin molecule via the mirror-symmetrical concerted rotations of the O3′H and O4′H hydroxyl groups around the C3′-O3′ and C4′-O4′ bonds through the non-planar or locally non-planar transition states (TSs), obtained at the MP2/6-311++G(2df,pd)//B3LYP/6-311++G(d,p) level of QM theory under normal conditions (see Figure 3).

TS of the Conformational Transition	μ_{TS}	ν_i	ΔG	ΔE	$\Delta\Delta G_{TS}$	$\Delta\Delta E_{TS}$	ΔΔG	ΔΔE	k_f	k_r	$\tau_{99.9\%}$	τ	HO3′C3′C4′/HO4′C4′C3′
$TS^{O3'H/O4'H}{}_{1\leftrightarrow7}$	2.97	457.1	0.92	1.09	7.50	7.99	6.59	6.90	$2.31{\cdot}10^{7}$	$1.09{\cdot}10^{8}$	$5.23{\cdot}10^{-8}$	$9.17{\cdot}10^{-9}$	±12.5/∓14.4
$TS^{O3'H/O4'H}{}_{2\leftrightarrow3}$	3.73	470.5	0.07	-0.23	7.03	7.19	6.96	7.42	$5.16{\cdot}10^{7}$	$5.80{\cdot}10^{7}$	$6.30{\cdot}10^{-8}$	$1.72{\cdot}10^{-8}$	±12.3/∓14.1
$TS^{O3'H/O4'H}{}_{4\leftrightarrow6}$	6.15	467.7	0.27	0.07	7.18	7.19	6.91	7.12	$4.04{\cdot}10^{7}$	$6.38{\cdot}10^{7}$	$6.63{\cdot}10^{-8}$	$1.57{\cdot}10^{-8}$	±12.5/∓14.3
$TS^{O3'H/O4'H}{}_{5\leftrightarrow8}$	5.56	459.1	0.92	1.14	7.40	7.96	6.48	6.82	$2.74{\cdot}10^{7}$	$1.29{\cdot}10^{8}$	$4.41{\cdot}10^{-8}$	$7.73{\cdot}10^{-9}$	±12.4/∓14.3
$TS^{O3'H/O4'H}{}_{13\leftrightarrow14}$	6.37	483.1	0.37	0.37	6.56	7.55	6.19	7.18	$1.16{\cdot}10^{8}$	$2.17{\cdot}10^{8}$	$2.07{\cdot}10^{-8}$	$4.61{\cdot}10^{-9}$	±8.3/∓9.3
$TS^{O3'H/O4'H}{}_{15\leftrightarrow20}$	6.09	466.9	3.13	3.25	6.30	7.13	3.17	3.88	$1.79{\cdot}10^{8}$	$3.53{\cdot}10^{10}$	$1.95{\cdot}10^{-10}$	$2.83{\cdot}10^{-11}$	±10.0/∓12.3
$TS^{O3'H/O4'H}{}_{16\leftrightarrow18}$	8.76	469.1	0.22	0.17	6.49	7.26	6.27	7.09	$1.29{\cdot}10^{8}$	$1.88{\cdot}10^{8}$	$2.18{\cdot}10^{-8}$	$5.31{\cdot}10^{-9}$	±9.1/∓11.3
$TS^{O3'H/O4'H}{}_{17\leftrightarrow23}$	8.97	473.2	3.25	3.31	6.32	7.21	3.07	3.90	$1.73{\cdot}10^{8}$	$4.19{\cdot}10^{10}$	$1.64{\cdot}10^{-10}$	$2.39{\cdot}10^{-11}$	±10.3/∓11.2
$TS^{O3'H/O4'H}{}_{19\leftrightarrow27}$	4.38	455.1	0.87	1.46	7.46	8.11	6.59	6.64	$2.50{\cdot}10^{7}$	$1.09{\cdot}10^{8}$	$5.17{\cdot}10^{-8}$	$9.20{\cdot}10^{-9}$	±13.9/∓15.6
$TS^{O3'H/O4'H}{}_{21\leftrightarrow22}$	5.41	461.5	0.03	0.17	6.75	7.21	6.72	7.04	$8.30{\cdot}10^{7}$	$8.73{\cdot}10^{7}$	$4.06{\cdot}10^{-8}$	$1.15{\cdot}10^{-8}$	±14.1/∓15.6
$TS^{O3'H/O4'H}{}_{25\leftrightarrow32}$	3.43	454.5	0.86	1.29	7.56	8.08	6.70	6.78	$2.11{\cdot}10^{7}$	$9.02{\cdot}10^{7}$	$6.21{\cdot}10^{-8}$	$1.11{\cdot}10^{-8}$	±14.0/∓15.8
$TS^{O3'H/O4'H}{}_{28\leftrightarrow31}$	4.51	465.7	0.22	0.20	6.89	7.34	6.67	7.14	$6.56{\cdot}10^{7}$	$9.50{\cdot}10^{7}$	$4.30{\cdot}10^{-8}$	$1.05{\cdot}10^{-8}$	±13.8/∓15.3
$TS^{O3'H/O4'H}{}_{37\leftrightarrow39}$	7.18	468.7	6.58	7.32	6.58	7.32	6.38	7.19	$1.11{\cdot}10^{8}$	$1.55{\cdot}10^{8}$	$2.60{\cdot}10^{-8}$	$6.46{\cdot}10^{-9}$	±12.3/∓13.0
$TS^{O3'H/O4'H}{}_{38\leftrightarrow40}$	6.91	470.9	0.33	0.33	6.56	7.36	6.23	7.03	$1.14{\cdot}10^{8}$	$2.01{\cdot}10^{8}$	$2.19{\cdot}10^{-8}$	$4.98{\cdot}10^{-9}$	±9.6/∓11.7
$TS^{O3'H/O4'H}{}_{41\leftrightarrow42}$	4.74	467.2	0.30	0.25	6.56	7.33	6.26	7.07	$1.15{\cdot}10^{8}$	$1.90{\cdot}10^{8}$	$2.27{\cdot}10^{-8}$	$5.26{\cdot}10^{-9}$	±10.7/∓12.9
$TS^{O3'H/O4'H}{}_{43\leftrightarrow44}$	5.12	476.2	0.37	0.37	4.41	5.29	4.04	4.92	$4.37{\cdot}10^{9}$	$8.13{\cdot}10^{9}$	$5.53{\cdot}10^{-10}$	$1.23{\cdot}10^{-10}$	±10.6/∓11.3

For designations see Table 1.

2 ⇿ 9			**21 ⇿ 34**		
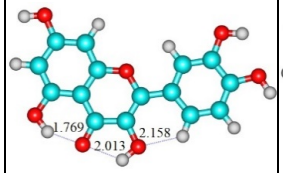	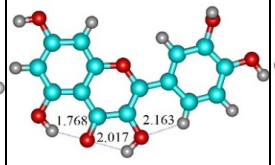	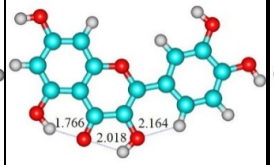	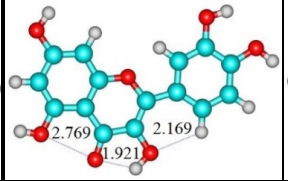	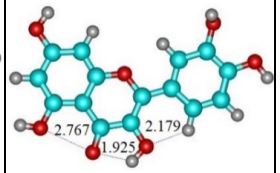	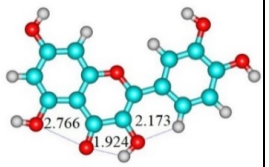
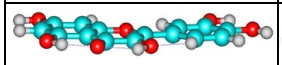	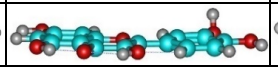	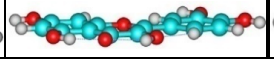	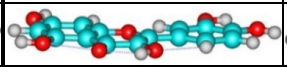	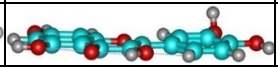	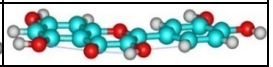
2 *(ΔG=0.18 / ΔE=0.78/μ=2.71)* *(ΔG$_{TS}$=0.00 / ΔE$_{TS}$=0.00)*	**TS$^{O3'H}{}_{2⇿9}$** *(ν_i=340.2 cm^{-1})* *(ΔG=7.08 / ΔE=7.53/ μ=1.78)* *(ΔG$_{TS}$=6.90 / ΔE$_{TS}$=6.75)*	**9** *(ΔG=4.17 / ΔE=4.58/μ=1.41)* *(ΔG$_{TS}$=3.98 / ΔE$_{TS}$=3.80)*	**21** (ΔG=11.52 / ΔE=12.53/μ=3.09) *(ΔG$_{TS}$=0.00 / ΔE$_{TS}$=0.00)*	**TS$^{O3'H}{}_{21⇿34}$** (ν_i=328.8 cm^{-1}) (ΔG=18.06 / ΔE=19.23/ μ=3.08) *(ΔG$_{TS}$=6.54 / ΔE$_{TS}$=6.70)*	**34** (ΔG=15.53 / ΔE=16.67/μ=3.71) *(ΔG$_{TS}$=4.01 / ΔE$_{TS}$=4.14)*
4 ⇿ 11			**27 ⇿ 33**		
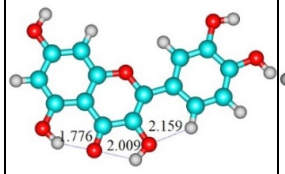	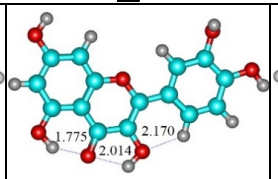	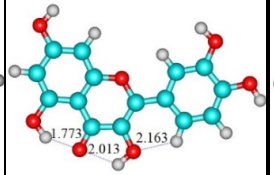	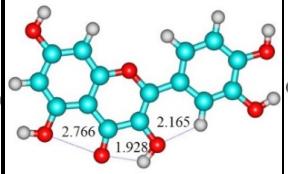	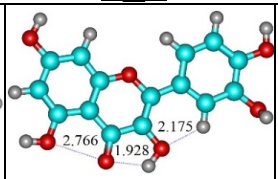	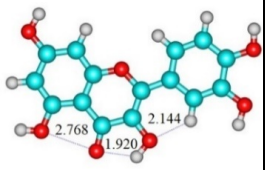
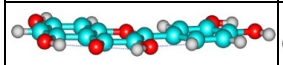	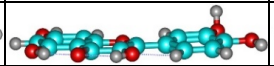	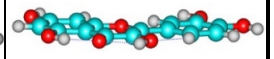	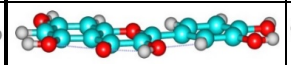	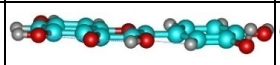	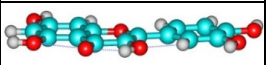
4 *(ΔG=0.26 / ΔE=1.01/μ=5.33)* *(ΔG$_{TS}$=0.00 / ΔE$_{TS}$=0.00)*	**TS$^{O3'H}{}_{4⇿11}$** *(ν_i=333.4 cm^{-1})* *(ΔG=7.32 / ΔE=7.75/ μ=4.02)* *(ΔG$_{TS}$=7.08 / ΔE$_{TS}$=6.73)*	**11** *(ΔG=4.39 / ΔE=5.08/μ=3.66)* *(ΔG$_{TS}$=4.15 / ΔE$_{TS}$=4.07)*	**27** (ΔG=11.95 / ΔE=13.12/μ=6.97) *(ΔG$_{TS}$=0.00 / ΔE$_{TS}$=0.00)*	**TS$^{O3'H}{}_{27⇿33}$** (ν_i=363.5 cm^{-1}) (ΔG=18.22 / ΔE=19.42 / μ=6.23) *(ΔG$_{TS}$=6.27 / ΔE$_{TS}$=6.29)*	**33** (ΔG=15.20 / ΔE=16.15/μ=5.37) *(ΔG$_{TS}$=3.25 / ΔE$_{TS}$=3.03)*

Figure 1. *Cont.*

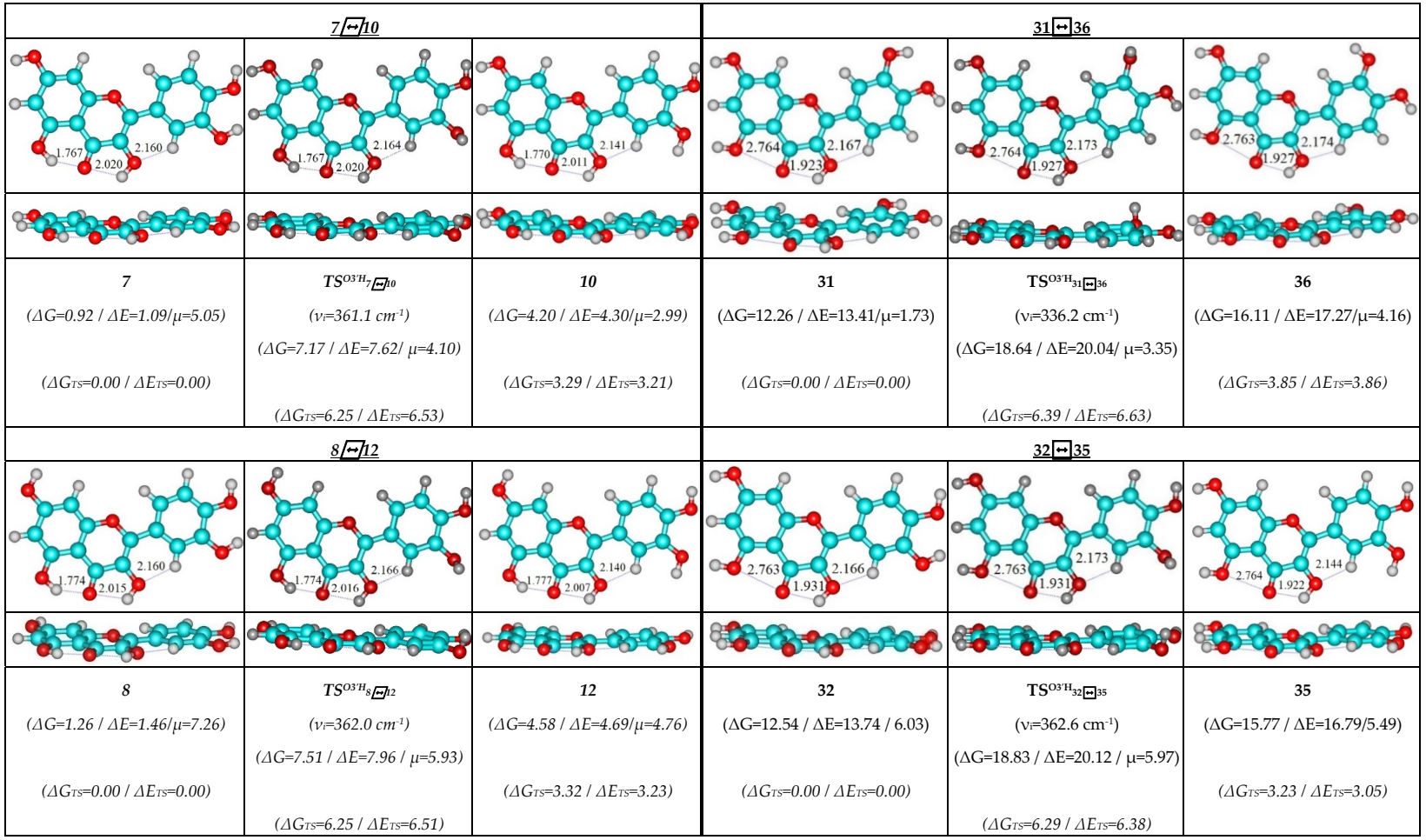

Figure 1. *Cont.*

14 ⇿ ***24***			**39** ⇿ **45**		
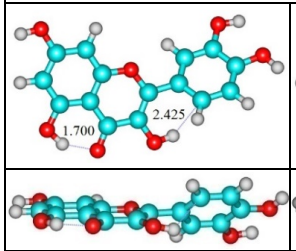	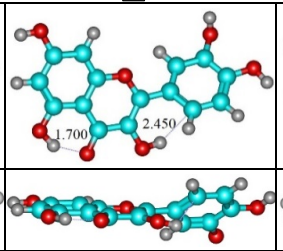	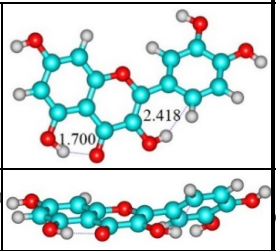	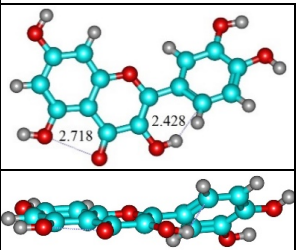	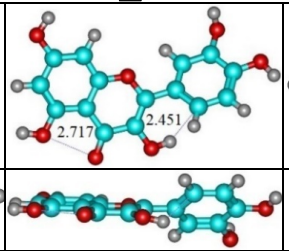	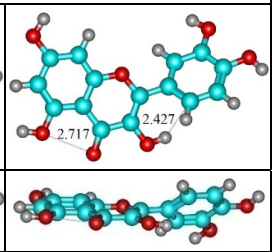
14	***TS$^{O3'H}_{14⇿24}$***	***24***	**39**	**TS$^{O3'H}_{39⇿45}$**	**45**
(ΔG=7.96 / ΔE=8.03 / 5.96)	*(ν_i=355.2 cm^{-1})*	*(ΔG=11.66 / ΔE=11.79/4.07)*	(ΔG=20.98 / ΔE=22.05/μ=6.28)	(ν_i=354.7 cm^{-1})	(ΔG=24.81 / ΔE=25.97/μ=5.30)
(ΔG_{TS}=0.00 / ΔE_{TS}=0.00)	*(ΔG=14.47 / ΔE=14.96/ μ=5.08)*	*(ΔG_{TS}=3.70 / ΔE_{TS}=3.75)*	*(ΔG_{TS}=0.00 / ΔE_{TS}=0.00)*	(ΔG=27.58 / ΔE=29.06/ μ=6.15)	*(ΔG_{TS}=3.83 / ΔE_{TS}=3.92)*
	(ΔG_{TS}=6.50 / ΔE_{TS}=6.92)			*(ΔG_{TS}=6.60 / ΔE_{TS}=7.01)*	
15 ⇿ ***26***			**40** ⇿ **46**		
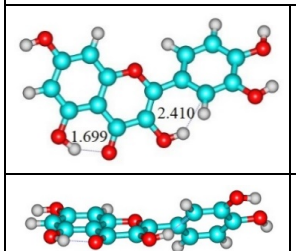	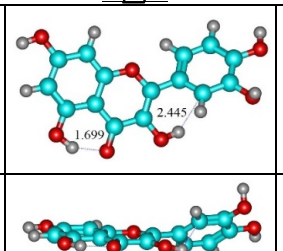	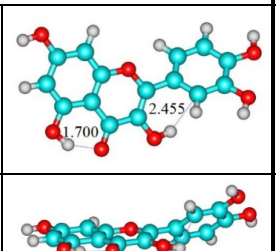	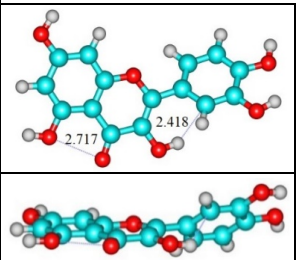	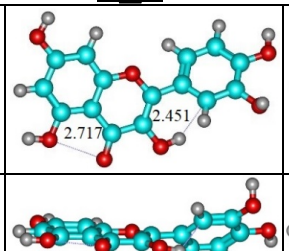	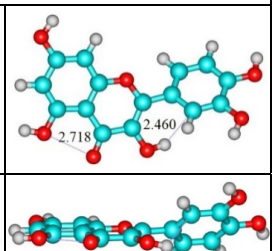
15	***TS$^{O3'H}_{15⇿26}$***	***26***	**40**	**TS$^{O3'H}_{40⇿46}$**	**46**
(ΔG=7.98 / ΔE=8.15/μ=7.35)	*(ν_i=340.9 cm^{-1})*	*(ΔG=11.74 / ΔE=12.12/μ=4.79)*	(ΔG=21.17/ΔE=22.36/μ=8.50)	(ν_i=344.1 cm^{-1})	(ΔG=24.87/ΔE=26.18/μ=6.29)
(ΔG_{TS}=0.00 / ΔE_{TS}=0.00)	*(ΔG=14.42 / ΔE=15.01 / μ=6.24)*	*(ΔG_{TS}=3.79 / ΔE_{TS}=3.97)*	*(ΔG_{TS}=0.00 / ΔE_{TS}=0.00)*	(ΔG=27.62 / ΔE=29.16/ μ=7.86)	*(ΔG_{TS}=3.70 / ΔE_{TS}=3.82)*
	(ΔG_{TS}=6.47 / ΔE_{TS}=6.86)			*(ΔG_{TS}=6.45 / ΔE_{TS}=6.80)*	

Figure 1. *Cont.*

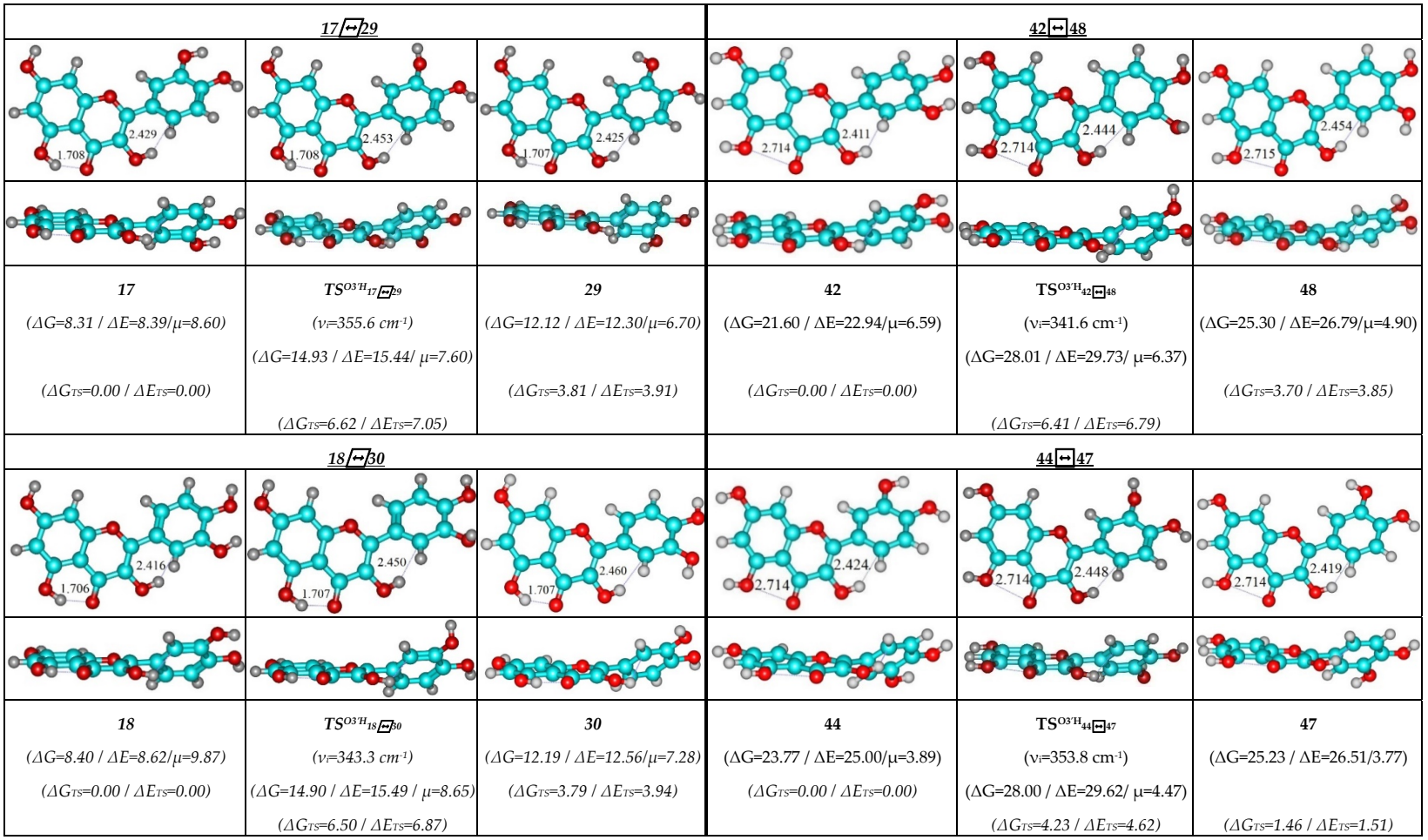

Figure 1. Geometrical structures of the quercetin molecule conformers and TSs with non-perpendicularly-oriented hydroxyl groups of their mutual interconversions via the mirror-symmetrical rotation of the O3'H hydroxyl group around the C3'-O3' bonds, obtained at the MP2/6-311++G(2df,pd)//B3LYP/6-311++G(d,p) level of QM theory under normal conditions. Relative Gibbs free ΔG and electronic ΔE energies (in kcal·mol^{-1}) (upper row represents energies relatively the conformer **1**, whereas the lower row presents the initial conformer for each transformation), dipole moments μ (Debye), and imaginary frequencies at TSs are provided at the MP2/6-311++G(2df,pd)//B3LYP/6-311++G(d,p) level of QM theory). Dotted lines indicate specific intramolecular contacts; their lengths are presented in Angstrom.

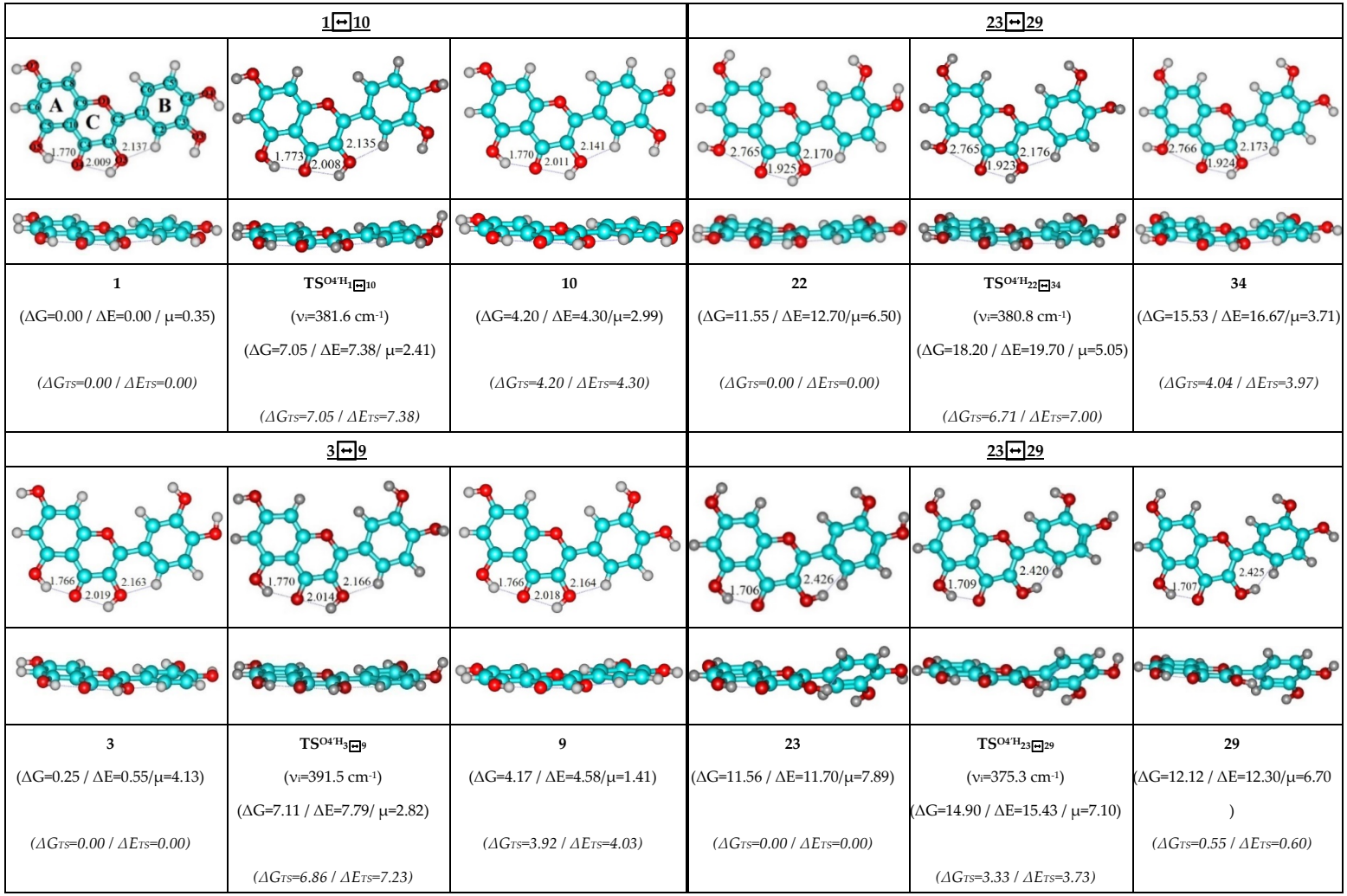

Figure 2. *Cont.*

5↔12			**25↔35**		
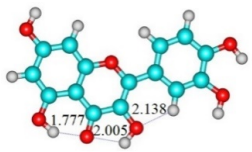	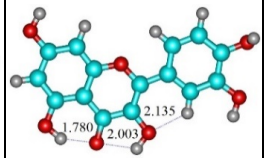	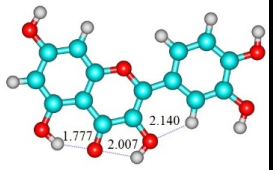	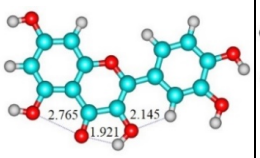	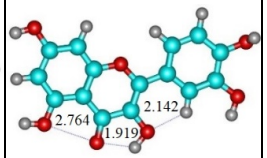	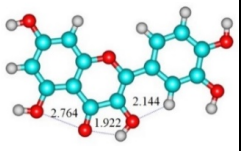
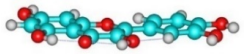	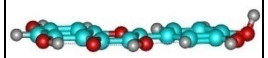	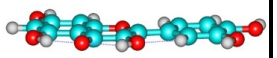	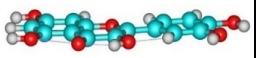	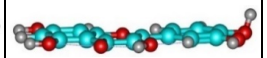	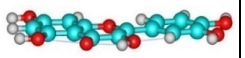
5	**$TS^{O4'H}_{5↔12}$**	**12**	**25**	**$TS^{O4'H}_{25↔35}$**	**35**
(ΔG=0.34 / ΔE=0.32/ μ=3.01)	(ν_i=379.7 cm^{-1})	(ΔG=4.58 / ΔE=4.69/μ=4.76)	(ΔG=11.68 / ΔE=12.45/μ=3.55)	(ν_i=373.7 cm^{-1})	(ΔG=15.77 / ΔE=16.79/5.49)
(ΔG_{TS}=0.00 / ΔE_{TS}=0.00)	(ΔG=7.27 / ΔE=7.67 / μ=3.63)	*(ΔG_{TS}=4.24 / ΔE_{TS}=4.37)*	*(ΔG_{TS}=0.00 / ΔE_{TS}=0.00)*	(ΔG=18.48 / ΔE=19.67/ μ=5.37)	*(ΔG_{TS}=4.12 / ΔE_{TS}=4.35)*
	(ΔG_{TS}=6.93 / ΔE_{TS}=7.35)			*(ΔG_{TS}=6.84 / ΔE_{TS}=7.22)*	
6↔11			**28↔36**		
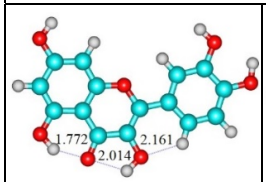	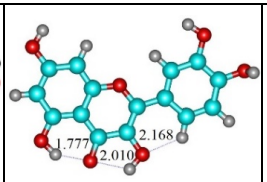	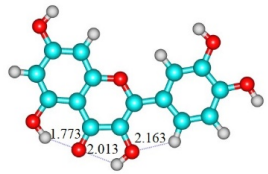	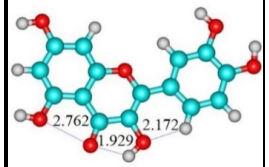	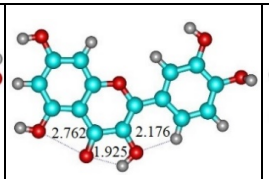	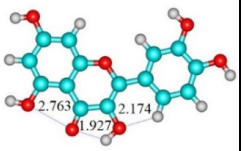
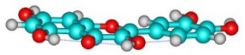	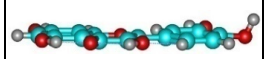	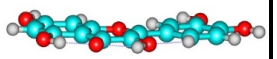	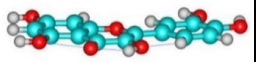	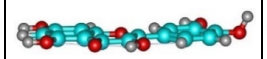	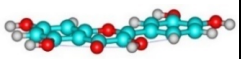
6	**$TS^{O4'H}_{6↔11}$**	**11**	**28**	**$TS^{O4'H}_{28↔36}$**	**36**
(ΔG=0.53 / ΔE=1.08 / μ=5.65)	(ν_i=389.2 cm^{-1})	(ΔG=4.39 / ΔE=5.08/μ=3.66)	(ΔG=12.04 / ΔE=13.21/μ=6.54)	(ν_i=382.7 cm^{-1})	(ΔG=16.11 / ΔE=17.27/μ=4.16)
(ΔG_{TS}=0.00 / ΔE_{TS}=0.00)	(ΔG=7.45 / ΔE=8.22/ μ=3.99)	*(ΔG_{TS}=3.86 / ΔE_{TS}=4.00)*	*(ΔG_{TS}=0.00 / ΔE_{TS}=0.00)*	(ΔG=18.78 / ΔE=20.29 / μ=5.70)	*(ΔG_{TS}=4.07 / ΔE_{TS}=4.06)*
	(ΔG_{TS}=6.92 / ΔE_{TS}=7.14)			*(ΔG_{TS}=6.74 / ΔE_{TS}=7.08)*	

Figure 2. *Cont.*

13↔24			**37↔45**		
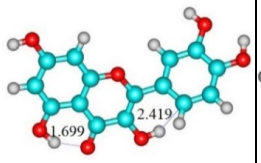	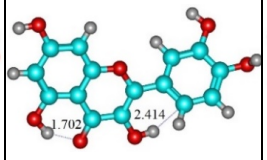	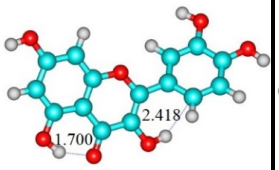	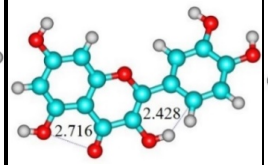	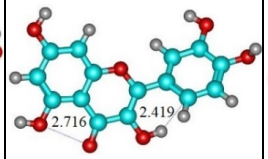	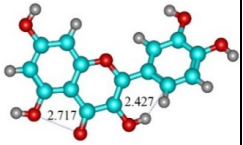
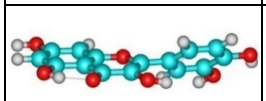	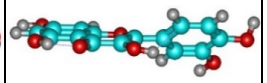	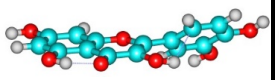	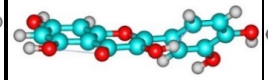	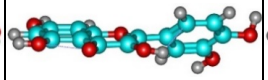	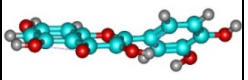
13 (ΔG=7.59 / ΔE=7.66/μ=5.64) *(ΔG$_{TS}$=0.00 / ΔE$_{TS}$=0.00)*	**TS$^{O4'H}_{13↔24}$** (ν_i=375.8 cm^{-1}) (ΔG=14.40 / ΔE=14.88 / μ=4.78) *(ΔG$_{TS}$=6.81 / ΔE$_{TS}$=7.22)*	**24** (ΔG=11.66 / ΔE=11.79/4.07) *(ΔG$_{TS}$=4.07 / ΔE$_{TS}$=4.13)*	**37** (ΔG=20.78 / ΔE=21.92/μ=7.22) *(ΔG$_{TS}$=0.00 / ΔE$_{TS}$=0.00)*	**TS$^{O4'H}_{37↔45}$** (ν_i=369.1 cm^{-1}) (ΔG=27.53 / ΔE=29.03/ μ=6.56) *(ΔG$_{TS}$=6.75 / ΔE$_{TS}$=7.11)*	**45** (ΔG=24.81 / ΔE=25.97/μ=5.30) *(ΔG$_{TS}$=4.03 / ΔE$_{TS}$=4.05)*
16↔30			**38↔46**		
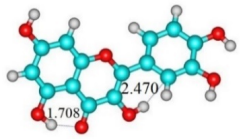	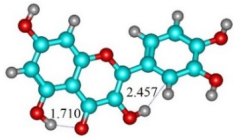	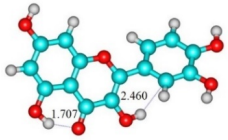	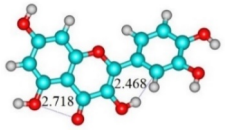	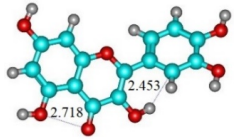	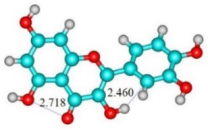
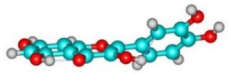	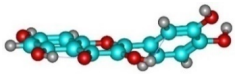	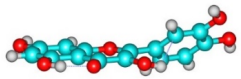	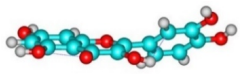	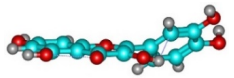	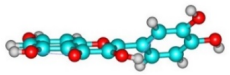
16 (ΔG=8.18/ΔE=8.45/μ=6.24) *(ΔG$_{TS}$=0.00 / ΔE$_{TS}$=0.00)*	**TS$^{O3'H}_{16↔30}$** (ν_i=374.4 cm^{-1}) (ΔG=14.96 / ΔE=15.60/ μ=6.83) *(ΔG$_{TS}$=6.78 / ΔE$_{TS}$=7.16)*	**30** (ΔG=12.19 / ΔE=12.56/μ=7.28) *(ΔG$_{TS}$=4.01 / ΔE$_{TS}$=4.11)*	**38** (ΔG=20.84 / ΔE=22.03 / μ=4.53)	**TS$^{O4'H}_{38↔46}$** (ν_i=367.5 cm^{-1}) (ΔG=27.56 / ΔE=29.13/ μ=6.19) *(ΔG$_{TS}$=6.72 / ΔE$_{TS}$=7.10)*	**46** (ΔG=24.87/ΔE=26.18/μ=6.29)

Figure 2. *Cont.*

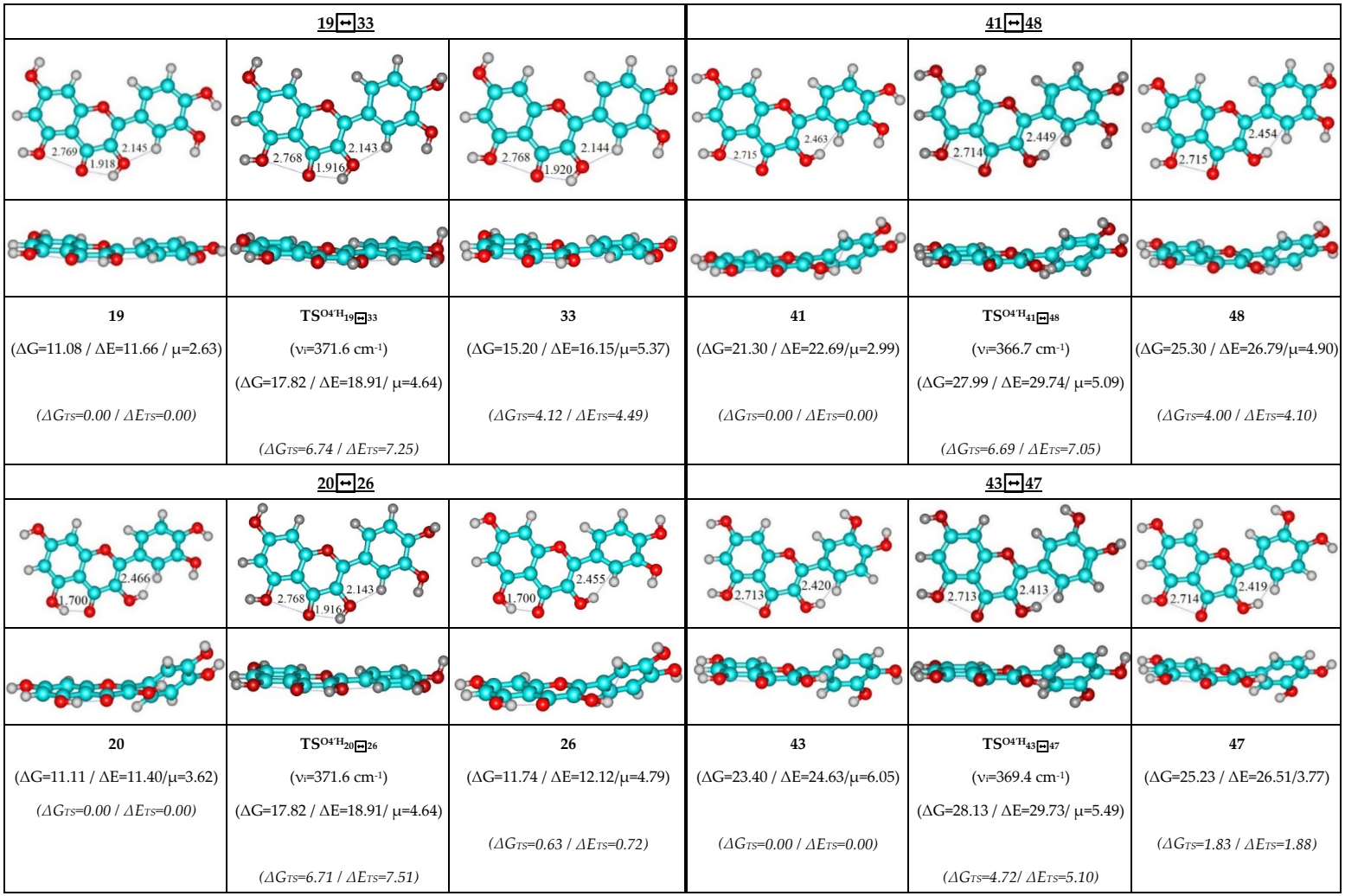

Figure 2. Geometrical structures of the quercetin molecule conformers and TSs with a non-perpendicularly-oriented hydroxyl groups of their mutual interconversions via the mirror-symmetrical rotation of the O4'H hydroxyl group around the C4'-O4' bond, obtained at the MP2/6-311++G(2df,pd)//B3LYP/6-311++G(d,p) level of QM theory under normal conditions. For designations see Figure 1.

1↔7			**19↔27**		
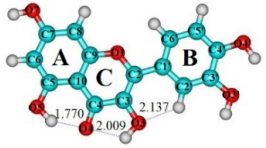	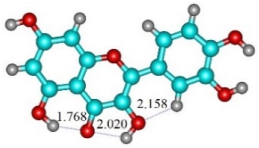	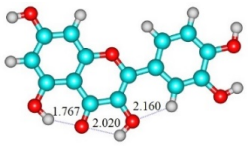	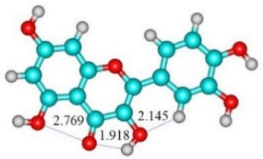	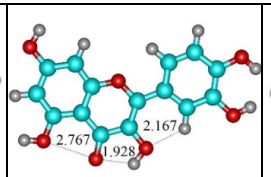	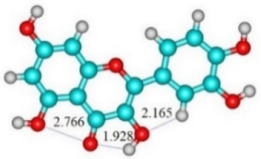
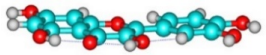	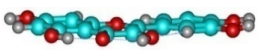	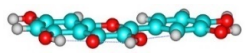	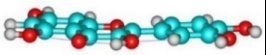	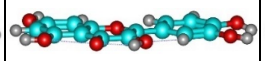	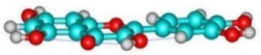
1 (ΔG=0.00 / ΔE=0.00 / μ=0.35)	**TS$^{O3'H/O4'H}_{1↔7}$** (ν_i=457.1 cm^{-1}) (ΔG=7.50 / ΔE=7.99/ μ=2.97)	**7** (ΔG=0.92 / ΔE=1.09/μ=5.05)	**19** (ΔG=11.08 / ΔE=11.66 / μ=2.63) *(ΔG_{TS}=0.00 / ΔE_{TS}=0.00)*	**TS$^{O3'H/O4'H}_{19↔27}$** (ν_i=455.1 cm^{-1}) (ΔG=18.54 / ΔE=19.77 / μ=4.38) *(ΔG_{TS}=7.46 / ΔE_{TS}=8.11)*	**27** (ΔG=11.95 / ΔE=13.12/μ=6.97) *(ΔG_{TS}=0.87 / ΔE_{TS}=1.46)*
2↔3			**21↔22**		
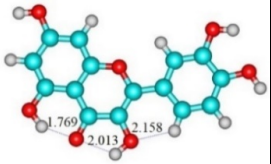	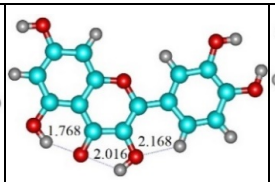	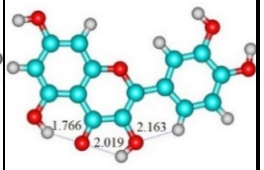	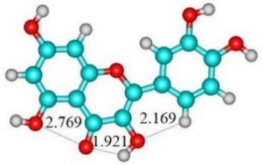	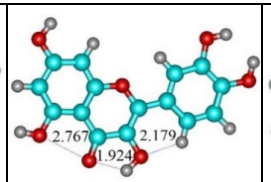	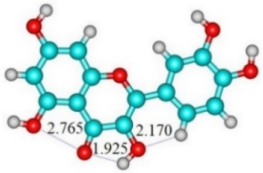
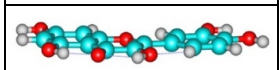	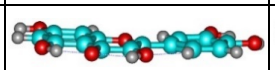	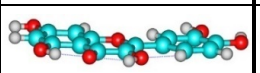	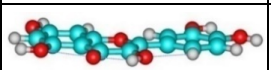	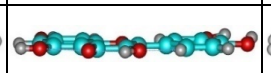	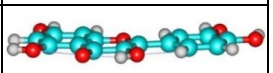
2 (ΔG=0.18 / ΔE=0.78/μ=2.71) *(ΔG_{TS}=0.00 / ΔE_{TS}=0.00)*	**TS$^{O3'H/O4'H}_{2↔3}$** (ν_i=470.5 cm^{-1}) (ΔG=7.22 / ΔE=7.7.97/ μ=3.73) *(ΔG_{TS}=7.03 / ΔE_{TS}=7.19)*	**3** (ΔG=0.25 / ΔE=0.55/μ=4.13) *(ΔG_{TS}=0.07 / ΔE_{TS}=−0.23)*	**21** (ΔG=11.52 / ΔE=12.53/μ=3.09) *(ΔG_{TS}=0.00 / ΔE_{TS}=0.00)*	**TS$^{O3'H/O4'H}_{21↔22}$** (ν_i=461.5 cm^{-1}) (ΔG=18.27 / ΔE=19.74 / μ=5.41) *(ΔG_{TS}=6.75 / ΔE_{TS}=7.21)*	**22** (ΔG=11.55 / ΔE=12.70/μ=6.50) *(ΔG_{TS}=0.03 / ΔE_{TS}=0.17)*

Figure 3. *Cont.*

4↔6			**25↔32**		
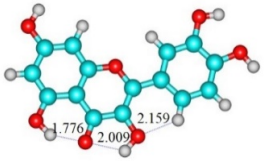	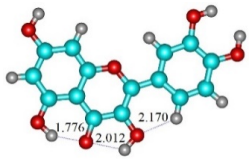	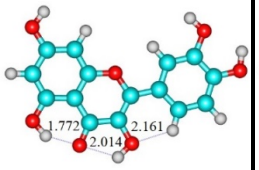	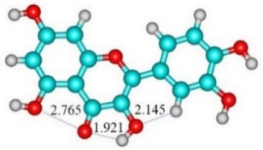	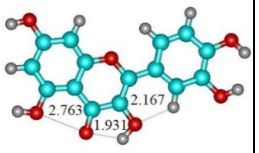	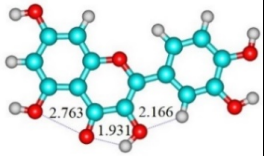
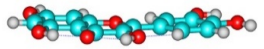	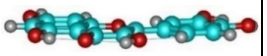	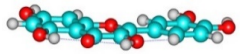	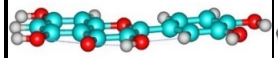	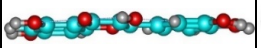	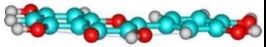
4 (ΔG=0.26 / ΔE=1.01/μ=5.33) *(ΔG$_{TS}$=0.00 / ΔE$_{TS}$=0.00)*	**TS$^{O3'H/O4'H}_{4↔6}$** (ν_i=467.7 cm^{-1}) (ΔG=7.42 / ΔE=8.21/ μ=6.15) *(ΔG$_{TS}$=7.18 / ΔE$_{TS}$=7.19)*	**6** (ΔG=0.53 / ΔE=1.08 / μ=5.65) *(ΔG$_{TS}$=0.27 / ΔE$_{TS}$=0.07)*	**25** (ΔG=11.68 / ΔE=12.45/μ=3.55) *(ΔG$_{TS}$=0.00 / ΔE$_{TS}$=0.00)*	**TS$^{O3'H/O4'H}_{25↔32}$** (ν_i=454.5 cm^{-1}) (ΔG=19.20 / ΔE=20.52 / μ=3.43) *(ΔG$_{TS}$=7.56 / ΔE$_{TS}$=8.08)*	**32** (ΔG=12.54 / ΔE=13.74 / 6.03) *(ΔG$_{TS}$=0.86 / ΔE$_{TS}$=1.29)*
5↔8			**28↔31**		
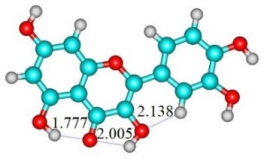	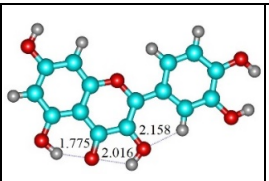	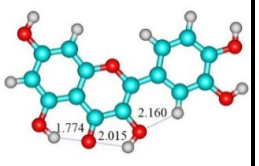	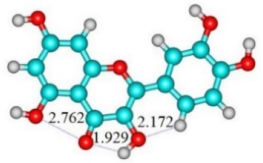	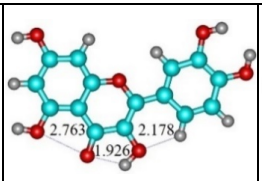	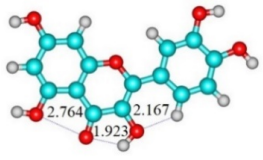
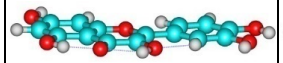	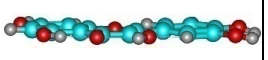	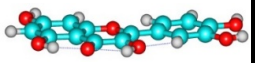	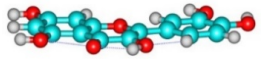	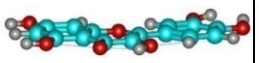	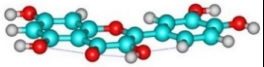
5 (ΔG=0.34 / ΔE=0.32/ μ=3.01) *(ΔG$_{TS}$=0.00 / ΔE$_{TS}$=0.00)*	**TS$^{O3'H/O4'H}_{5↔8}$** (ν_i=459.1 cm^{-1}) (ΔG=7.75 / ΔE=8.28 / μ=5.56) *(ΔG$_{TS}$=7.40 / ΔE$_{TS}$=7.96)*	**8** (ΔG=1.26 / ΔE=1.46/μ=7.26) *(ΔG$_{TS}$=0.92 / ΔE$_{TS}$=1.14)*	**28** (ΔG=12.04 / ΔE=13.21/μ=6.54) *(ΔG$_{TS}$=0.00 / ΔE$_{TS}$=0.00)*	**TS$^{O3'H/O4'H}_{28↔31}$** (ν_i=465.7 cm^{-1}) (ΔG=18.93 / ΔE=20.55 / μ=4.51) *(ΔG$_{TS}$=6.89 / ΔE$_{TS}$=7.34)*	**31** (ΔG=12.26 / ΔE=13.41/μ=1.73) *(ΔG$_{TS}$=0.22 / ΔE$_{TS}$=0.20)*

Figure 3. *Cont.*

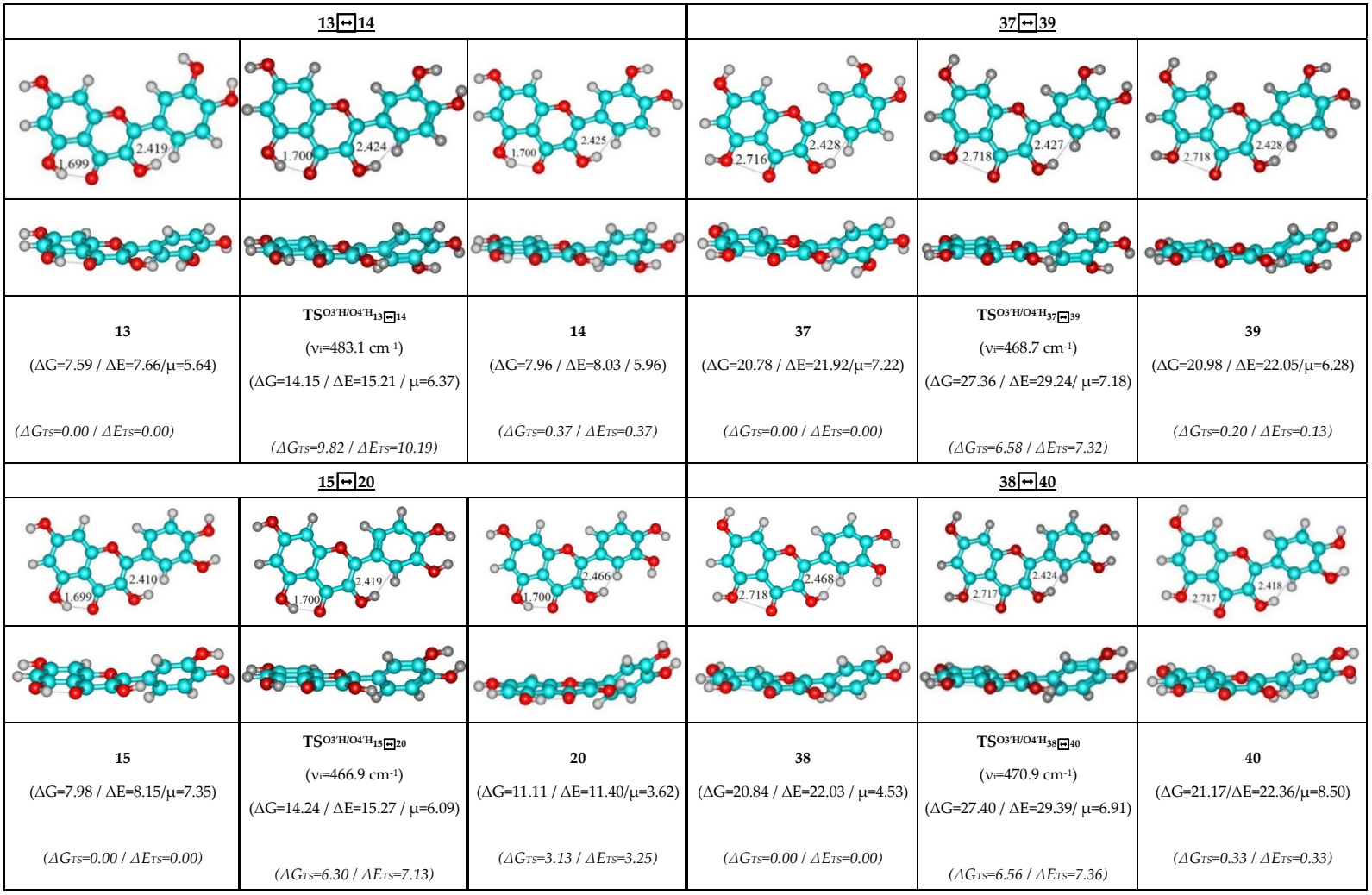

Figure 3. *Cont.*

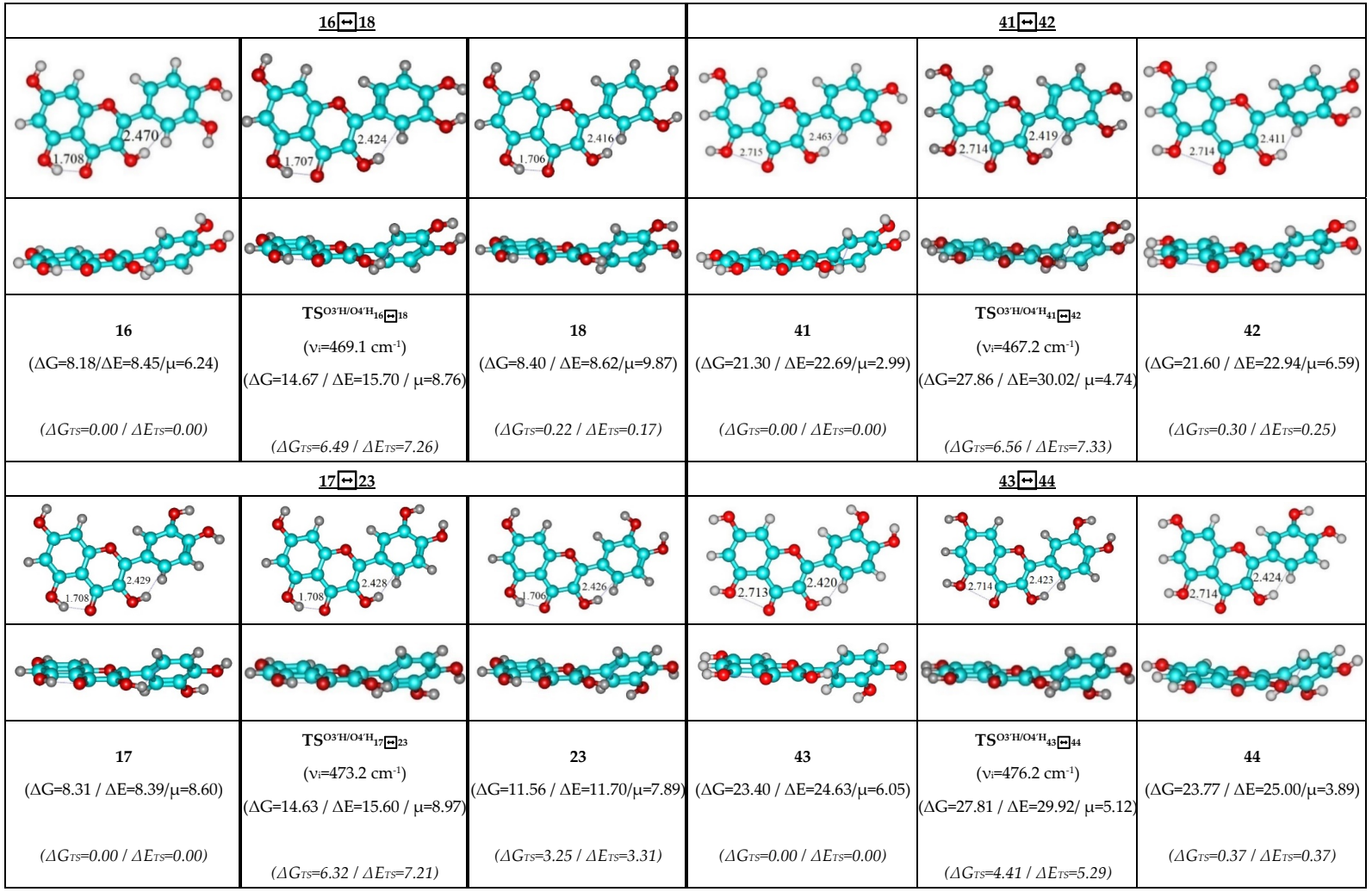

Figure 3. Geometrical structures of the quercetin molecule conformers and non-planar or locally non-planar TSs of their mutual concerted interconversions via the mirror-symmetrical rotation of the O3′H and O4′H hydroxyl groups around the C3′-O3′ and C4′-O4′ bonds, obtained at the MP2/6-311++G(2df,pd)//B3LYP/6-311++G(d,p) level of QM theory under normal conditions. For detailed designations see Figure 1.

In the case of the quercetin molecule, both of these tasks are overcomplicated. The reason is that the conformational mobility of this molecule is closely connected with its prototropic tautomerism [40,41]. It is known that the quercetin molecule has 202 molecular prototropic tautomers [40]. By contrast, now it is not known for sure all possible targets and their structure, despite all reasons to think that the range of this information would continuously grow together with the growing of the progress in bioinformatics and structural analysis. If also consider the conformationally-tautomeric variability of the targets, it would become clear that clarification of the structural grounds for the biological activity of the quercetin molecule is quite difficult task. We aimed to highlight this obstacle by the title of this paper.

4. Conclusions and Perspective for the Future Research

In this study, which is a logical continuation of our previous works on this topic [16–21], new pathways of the transformations of the conformers of the quercetin molecule into each other were found, which occurred due to the torsional mobility of the O3'H and O4'H hydroxyl groups.

It was established that the presence of only three degrees of freedom of the conformational mobility of the O3'H and O4'H hydroxyl groups is connected with their concerted behavior, which is controlled by the non-planar (in the case of the interconverting planar conformers) or locally non-planar (in other cases) $TSs^{O3'H/O4'H}$, in which O3'H and O4'H hydroxyl groups are oriented by the hydrogen atoms towards each other.

All these results assert that quercetin is a rather dynamical molecule, which is able to transform through the pathways into different conformers, forming complex networking.

We also shortly described the long-term perspectives for the investigation of the structural basis of the biological activity of quercetin.

Author Contributions: Setting of an idea of investigation, data preparation, analysis of the received results, writing and proofreading of the text of manuscript, references, Tables and Figures have been performed jointly by O.O.B. and D.M.H. All authors have read and agreed to the published version of the manuscript.

Funding: This research received no extra fuding.

Conflicts of Interest: The authors declare no conflict of interest.

References

1. Cianciosi, D.; Forbes-Hernández, T.Y.; Afrin, S.; Gasparrini, M.; Reboredo-Rodriguez, P.; Manna, P.P.; Zhang, J.; Lamas, L.B.; Flórez, S.M.; Toyos, P.A.; et al. Phenolic compounds in honey and their associated health benefits: A review. *Molecules* **2018**, *23*, 2322. [CrossRef] [PubMed]
2. Grytsenko, O.M.; Degtyarev, L.S.; Pilipchuck, L.B. Physico-chemical properties and electronic structure of quercetin. *Farmats. Zhurn.* **1992**, *N2*, 34–38.
3. Burda, S.; Oleszek, W. Antioxidant and antiradical activities of flavonoids. *J. Agric. Food Chem.* **2001**, *49*, 2774–2779. [CrossRef] [PubMed]
4. Grytsenko, O.M.; Pylypchuck, L.B.; Bogdan, T.V.; Trygubenko, S.A.; Hovorun, D.M.; Maksutina, N.P. Keto-enol prototropic tautomerism of quercetin molecule: Quantum-chemical calculations. *Farmats. Zhurn.* **2003**, *N5*, 62–65.
5. Olejniczak, S.; Potrzebowski, M.J. Solid state NMR studies and density functional theory (DFT) calculations of conformers of quercetin. *Org. Biomol. Chem.* **2004**, *2*, 2315–2322. [CrossRef]
6. Bentz, A.B. A review of quercetin: Chemistry, antioxidant properties, and bioavailability. *J. Young Investig.* **2009**, *19*, 1–14.
7. Tošović, J.; Marković, S.; Dimitrić Marković, J.M.; Mojović, M.; Milenković, D. Antioxidative mechanisms in chlorogenic acid. *Food Chem.* **2017**, *237*, 390–398. [CrossRef]
8. Nathiya, S.; Durga, M.; Devasena, T. Quercetin, encapsulated quercetin and its application—A review. *Int. J. Pharm. Pharm. Sci.* **2014**, *10*, 20–26.
9. David, A.V.A.; Arulmoli, R.; Parasuraman, S. Overviews of biological importance of quercetin: A bioactive flavonoid. *Pharmacogn. Rev.* **2016**, *10*, 84–89.

10. van Acker, S.A.; de Groot, M.J.; van den Berg, D.J.; Tromp, M.N.; Donné-Op den Kelder, G.; van der Vijgh, W.J.; Bast, A.A. A quantum chemical explanation of the antioxidant activity of flavonoids. *Chem. Res. Toxicol.* **1996**, *9*, 1305–1312. [CrossRef]
11. Bogdan, T.V.; Trygubenko, S.A.; Pylypchuck, L.B.; Potyahaylo, A.L.; Samijlenko, S.P.; Hovorun, D.M. Conformational analysis of the quercetin molecule. *Sci. Notes NaUKMA* **2001**, *19*, 456–460.
12. Trouillas, P.; Marsal, P.; Siri, D.; Lazzaroni, R.; Duroux, J.-C. A DFT study of the reactivity of OH groups in quercetin and taxifolin antioxidants: The specificity of the 3-OH site. *Food Chem.* **2006**, *97*, 679–688. [CrossRef]
13. Marković, Z.; Amić, D.; Milenković, D.; Dimitrić-Marković, J.M.; Marković, S. Examination of the chemical behavior of the quercetin radical cation towards some bases. *Phys. Chem. Chem. Phys.* **2013**, *15*, 7370–7378. [CrossRef] [PubMed]
14. Protsenko, I.O.; Hovorun, D.M. Conformational properties of quercetin: Quantum chemistry investigation. *Rep. Natl. Acad. Sci. Ukr.* **2014**, *N3*, 153–157. [CrossRef]
15. Vinnarasi, S.; Radhika, R.; Vijayakumar, S.; Shankar, R. Structural insights into the anti-cancer activity of quercetin on G-tetrad, mixed G-tetrad, and G-quadruplex DNA using quantum chemical and molecular dynamics simulations. *J. Biomol. Struct. Dyn.* **2019**. [CrossRef]
16. Brovarets', O.O.; Hovorun, D.M. Conformational diversity of the quercetin molecule: A quantum-chemical view. *J. Biomol. Struct. Dyn.* **2019**. [CrossRef]
17. Brovarets', O.O.; Hovorun, D.M. Conformational transitions of the quercetin molecule via the rotations of its rings: A comprehensive theoretical study. *J. Biomol. Struct. Dyn.* **2019**. [CrossRef]
18. Brovarets', O.O.; Hovorun, D.M. A hidden side of the conformational mobility of the quercetin molecule caused by the rotations of the O3H, O5H and O7H hydroxyl groups. In silico scrupulous study. *Symmetry* **2020**, *12*, 230.
19. Brovarets', O.O.; Protsenko, I.O.; Hovorun, D.M. Computational design of the conformational and tautomeric variability of the quercetin molecule. In Proceedings of the 6th Young Medicinal Chemist Symposium (EFMC-YMCS 2019, Athens, Greece, 5–6 September 2019; p. 50.
20. Brovarets', O.O.; Protsenko, I.O.; Hovorun, D.M. Comprehensive analysis of the potential energy surface of the quercetin molecule. In Proceedings of the "Bioheterocycles 2019" XVIII International Conference on Heterocycles in Bioorganic Chemistry, Ghent, Belgium, 17–20 June 2019; p. 84.
21. Brovarets', O.O.; Protsenko, I.O.; Zaychenko, G. Computational modeling of the tautomeric interconversions of the quercetin molecule. In Proceedings of the International Symposium EFMC-ACSMEDI Medicinal Chemistry Frontiers 2019, MedChemFrontiers 2019, Krakow, Poland, 10–13 June 2019; p. 114.
22. Filip, X.; Filip, C. Can the conformation of flexible hydroxyl groups be constrained by simple NMR crystallography approaches? The case of the quercetin solid forms. *Solid State Nucl. Magn. Reson.* **2015**, *65*, 21–28. [CrossRef]
23. Filip, X.; Miclaus, M.; Martin, F.; Filip, C.; Grosu, I.G. Optimized multi-step NMR-crystallography approach for structural characterization of a stable quercetin solvate. *J. Pharm. Biomed. Anal.* **2017**, *138*, 22–28. [CrossRef]
24. Tirado-Rives, J.; Jorgensen, W.L. Performance of B3LYP Density Functional Methods for a large set of organic molecules. *J. Chem. Theory Comput.* **2008**, *4*, 297–306. [CrossRef] [PubMed]
25. Parr, R.G.; Yang, W. *Density-Functional Theory of Atoms and Molecules*; Oxford University Press: Oxford, UK, 1989.
26. Lee, C.; Yang, W.; Parr, R.G. Development of the Colle-Salvetti correlation-energy formula into a functional of the electron density. *Phys. Rev. B* **1988**, *37*, 785–789. [CrossRef] [PubMed]
27. Frisch, M.J.; Trucks, G.W.; Schlegel, H.B.; Scuseria, G.E.; Robb, M.A.; Cheeseman, J.R.; Scalmani, G.; Barone, V.; Mennucci, B.; Petersson, G.A.; et al. *GAUSSIAN 09 (Revision B.01)*; Gaussian Inc.: Wallingford, CT, USA, 2010.
28. Brovarets', O.O.; Hovorun, D.M. Atomistic understanding of the C·T mismatched DNA base pair tautomerization via the DPT: QM and QTAIM computational approaches. *J. Comput. Chem.* **2013**, *34*, 2577–2590. [CrossRef] [PubMed]
29. Brovarets', O.O.; Tsiupa, K.S.; Hovorun, D.M. Non-dissociative structural transitions of the Watson-Crick and reverse Watson-Crick A·T DNA base pairs into the Hoogsteen and reverse Hoogsteen forms. *Sci. Rep.* **2018**, *8*, 10371.

30. Palafox, M.A. Molecular structure differences between the antiviral nucleoside analogue 5-iodo-2′-deoxyuridine and the natural nucleoside 2′-deoxythymidine using MP2 and DFT methods: Conformational analysis, crystal simulations, DNA pairs and possible behavior. *J. Biomol. Struct. Dyn.* **2014**, *32*, 831–851. [CrossRef]
31. Hratchian, H.P.; Schlegel, H.B. Finding minima, transition states, and following reaction pathways on *ab initio* potential energy surfaces. In *Theory and Applications of Computational Chemistry: The First 40 Years*; Dykstra, C.E., Frenking, G., Kim, K.S., Scuseria, G., Eds.; Elsevier: Amsterdam, The Netherlands, 2005; pp. 195–249.
32. Vásquez-Espinal, A.; Yañez, O.; Osorio, E.; Areche, C.; García-Beltrán, O.; Ruiz, L.M.; Cassels, B.K.; Tiznado, W. Theoretical study of the antioxidant activity of quercetin oxidation products. *Front. Chem.* **2019**, *7*, 818. [CrossRef]
33. Frisch, M.J.; Head-Gordon, M.; Pople, J.A. Semi-direct algorithms for the MP2 energy and gradient. *Chem. Phys. Lett.* **1990**, *166*, 281–289. [CrossRef]
34. Hariharan, P.C.; Pople, J.A. The influence of polarization functions on molecular orbital hydrogenation energies. *Theor. Chim. Acta* **1973**, *28*, 213–222. [CrossRef]
35. Krishnan, R.; Binkley, J.S.; Seeger, R.; Pople, J.A. Self-consistent molecular orbital methods. XX. A basis set for correlated wave functions. *J. Chem. Phys.* **1980**, *72*, 650–654. [CrossRef]
36. Atkins, P.W. *Physical Chemistry*; Oxford University Press: Oxford, UK, 1998.
37. Wigner, E. Über das Überschreiten von Potentialschwellen bei chemischen Reaktionen [Crossing of potential thresholds in chemical reactions]. *Zeits. Physik. Chem.* **1932**, *B19*, 203–216.
38. Keith, T.A. AIMAll (Version 10.07.01). 2010. Available online: aim.tkgristmill.com (accessed on 7 January 2020).
39. Matta, C.F.; Hernández-Trujillo, J. Bonding in polycyclic aromatic hydrocarbons in terms of the electron density and of electron delocalization. *J. Phys. Chem. A* **2003**, *107*, 7496–7504. [CrossRef]
40. Brovarets', O.O.; Hovorun, D.M. A new era of the prototropic tautomerism of the quercetin molecule: A QM/QTAIM computational advances. *J. Biomol. Struct. Dyn.* **2019**. [CrossRef]
41. Brovarets', O.O.; Hovorun, D.M. Intramolecular tautomerization of the quercetin molecule due to the proton transfer: QM computational study. *PLoS ONE* **2019**, *14*, e0224762. [CrossRef] [PubMed]